International Journal of
INTELLIGENT SYSTEMS AND APPLICATIONS IN ENGINEERING
ISSN:2147-6799 www.ijisae.org Original Research Paper

LSTM-ANN Intelligent Control Based on Space Vector Modulated DTC for Induction Motor Drive

Dharmistha V. Makwana[1], Nilam B. Panchal*[2], Vaibhavi M. Parmar[3], Parul A. Upadhyay[4], Mehulsinh G. Jadeja[5]

Submitted: 01/05/2024 **Revised:** 15/06/2024 **Accepted:** 25/06/2024

Abstract: DTC, or Direct Torque Control, is an intriguing control method for induction motor drives (IMD) due to its independence from machine rotor parameters. Despite its simplicity, DTC offers effective control of torque steady and transient states. Nevertheless, hysteresis comparators in DTC drives encounter the problem of excessive ripples in torque and inconsistent switching frequency. Conventional DTC, on the other hand, is plagued by significant torque and flux ripples. To tackle this challenge, the widely adopted approach is to incorporate Space Vector Modulation (SVM), which relies on the reference flux and torque. This research paper explores the implementation of LSTM-ANN controllers in conjunction with the SVM method for the inverter. The torque ripple is significantly reduced by the proposed DTC-SVM-IMD system based on LSTM-ANN. To achieve precise speed control, a Fuzzy-PI Controller is employed, while LSTM-ANN duty ratio control is utilized to minimize ripples in flux and torque. The controller's gains are updated by the LSTM-ANN's output, which receives accurate outputs from the speed error and its derivative. This online tuning ensures excellent control performance, even when there are parameter variations and drive non-linearity. The benefits enable the integration of DTC-SVM-IMD with LSTM-ANN for electric vehicles.

Keywords: *DTC, Induction Motor Drive, LSTM-ANN Controller, SVM.*

1. Introduction

DTC has garnered considerable interest in contemporary literature. The machine's torque and flux are directly controlled by utilizing the hysteresis band [1-3]. In case the stator flux strays from the hysteresis region, the inverter will modify its settings to guarantee that the flux aligns with the optimal path towards the target value. The concept of "DTC" originates from the capability to directly adjust the inverter settings according to the differences between the desired and calculated values of torque and flux. The primary objective of this control strategy is to reduce the errors in flux and torque within specified boundaries. Figure 1 illustrates the generalized diagram of the conventional SVM-DTC.

DTC offers several key benefits, including a robust and rapid torque response, as well as the elimination of the need for coordinate transformation, PWM generator, and current regulators [4-5]. Nevertheless, a major disadvantage of DTC lies in the existence of constant state ripples in flux and torque. These variations in torque and flux adversely affect the precision of speed estimation, leading to higher levels of acoustical noise and harmonic losses [6-7]. Ripples in torque and flux of DTC induction motor drive present a significant challenge due to the inability of the switching vectors to generate the exact stator voltage needed for desired variations in flux and torque. In the conventional DTC method, hysteresis comparators analyze the errors in flux and torque magnitude to determine the suitable stator voltage vector that should be applied to the terminals of IMD. The complex plane is divided into 6 number of sectors, and a switching table is established to obtain the necessary vector based on the outputs of the hysteresis comparators. Nevertheless, the formidable task of keeping the machine torque within the hysteresis bands becomes exceedingly difficult due to the swift time constants of stator dynamics [8-10]. This objective can be accomplished through two methods: either by enhancing the sampling frequency to increase the commutation losses, switching frequency, and computational requirements, or by employing multilevel devices.

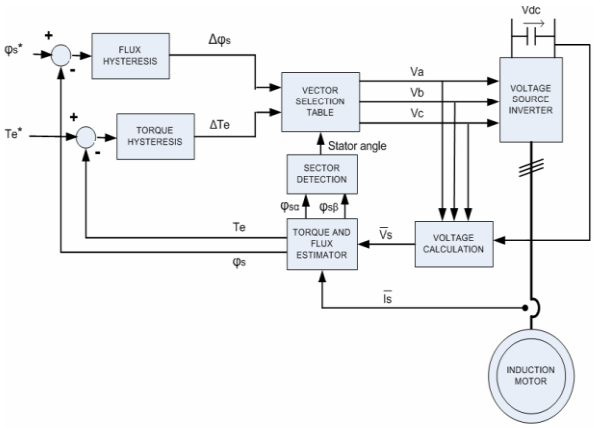

Fig. 1. DTC-SVM basic model.

The utilization of hysteresis band in traditional DTC implementations results in a fluctuating switching frequency, which is influenced by factors such as rotor speed, load, sample frequency, and more. The fluctuating switching frequency can lead

*1,*2,3,5 Electrical Engineering Department, Vishwakarma Government Engineering College, Chandkheda, Ahmedabad, Gujarat, India.*
ORCID ID: 10009-0005-3281-3297, 20009-0003-3746-0457, 30009-0007-2995-7462, 50009-0003-3945-8182
4Electrical Engineering Department, Government Engineering College, Bharuch, Gujarat, India.
4ORCID ID: 40000-0003-4190-4375
** Corresponding Author Email: nilam.b2211@gmail.com*

to the emergence of resonant dynamics in loads, thus posing a notable drawback of SVM-DTC.

There are typically two approaches available for reducing torque and flux ripple in DTC drives. The first method involves using a multi-level inverter, while the second method utilizes SVM [11-15]. The multi-level inverter method tends to increase both the cost and complexity of the system, whereas the SVM method can effectively reduce torque and flux ripple, although the switch frequency still varies. It is worth noting that most of these methods require significant computational resources. In the following section, an ANN based LSTM approach is proposed to address ripple reduction in torque. The optimal amplitude of the torque hysteresis band is established through the utilization of LSTM-ANN controllers.

2. Proposed Work

The implementation of a LSTM-ANN controller aims to improve the efficiency of the DTC scheme by minimizing the fluctuations in flux and torque. The conventional PI controllers employed are speed regulators that require a precise mathematical model of the system and appropriate values for the gains to attain optimal drive performances. However, any unforeseen variations in load conditions can lead to overshoot, motor speed oscillations, torque oscillations, prolonged settling time, and ultimately degrade the overall drive performances.

Throughout the entire switching cycle, the chosen voltage vector is consistently implemented, accommodating fluctuations in electromagnetic torque and stator flux over the entire duration. Consequently, this leads to significant fluctuations in flux and torque. In order to address these issues in DTC, three LSTM-ANN controllers have been extensively examined in various literature sources.

Figure 2 illustrates the depicted DTC-SVM with LSTM-ANN systems. The implementation of LSTM-ANN Logic in the online adjustment of the PI controller includes the reception of scaled values for both the speed error and the rate of change of speed error. Subsequently, the parameters of LSTM-ANN controller are adjusted based on trail ad error method, ensuring exceptional control performance despite parameter variation and non-linear drive.

Figure 2 depicts the block diagram showcasing the utilization of closed-loop flux and torque control within the stator flux coordinated model. The LSTM-ANN torque and flux controllers' results can be used to derive the reference stator voltage components. Terms V_{sy} *and* V_{sx}, are the coordinates of stator flux. We are able to achieve satisfactory speed and torque responses by employing three LSTM-ANN controllers. The outputs of these controllers are converted from X-Y to α-β coordinate components, resulting in Vsx and Vsy. Subsequently, we utilize these values to generate six switching states through the implementation of SVM, as detailed in section III.

3. DTC of IMD

To attain the intended stator flux, it is imperative to meticulously choose the appropriate state of the VSI. If we simplify the situation by disregarding the ohmic drops, it is important to note that the voltage of stator directly impacts the flux, as indicated by equations 1 and 2.

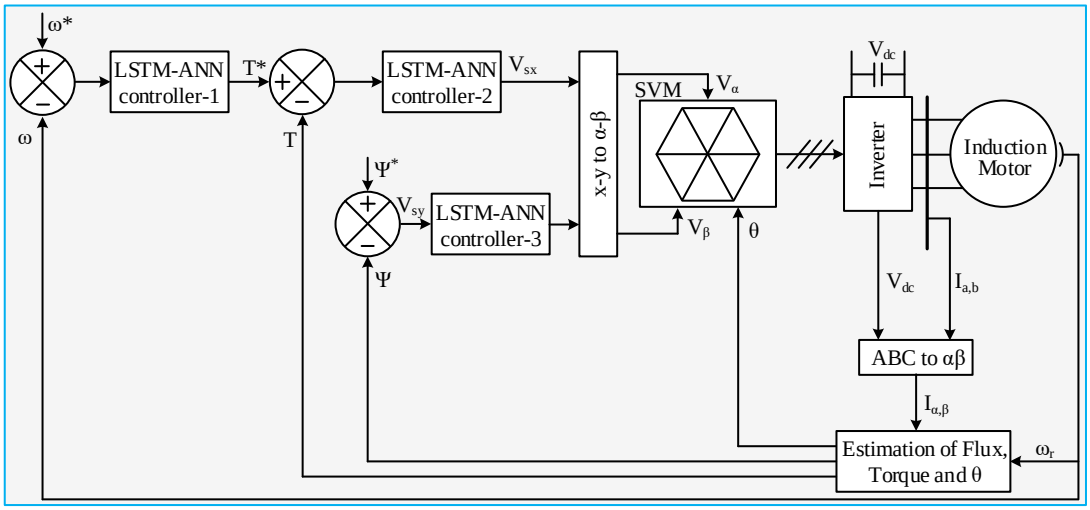

Fig. 2. LSTM-ANN controllers-based DTC-SVM model.

$$\frac{d\overline{\psi}_s}{dt} = \overline{u}_s \quad (1)$$

$$\Delta\overline{\psi}_s = \overline{u}_s \Delta t \quad (2)$$

It is possible to independently control the stator flux and torque by adjusting the tangential and radial components of the stator flux-linkage's vector. The elements are closely linked to the elements of the voltage vector in identical orientations. Figure 3 illustrates the fluctuations in the stator flux and its dynamics, which are contingent upon the selected VSI states. The stator flux of the global locus is partitioned into 6 sectors, denoted by the interrupted line.

Based on Figure 3, the comprehensive Table 1 can be derived. Table 1 demonstrates that the states V_{m+3} and V_m have no impact on the torque, as they can either amplify (during the initial 30^0) or reduce (during the subsequent 30^0) the torque within the identical sector, depending on the position of flux. The SVM is adopted from [13-15].

Table 1: DTC selection process being "m" the sector number.

Voltage Vector	Decrease	Increase
Torque	V_{m-2}; V_{m-1}.	V_{m+2}; V_{m+1}
Stator Flux	V_{m-2}; V_{m+2}; V_{m+3}.	V_{m-1}; V_m; V_{m+1}.

FI/FD stands for flux increase/decrease, while TI/T/TD stands for torque increase /equal/ decrease. S_x denotes the flux sector of stator winding. Φ represents the error module of stator flux following the hysteresis control, and τ denotes the torque error following the hysteresis control.

The stator flux SVM sectors are labeled as S_1 through S_6. The hysteresis block leads to two potential values for the error in stator flux modulus (Φ). On the other hand, the hysteresis system can result in three distinct values for the torque error (τ). Table 2 provides the necessary information regarding the selection and preservation of the zero voltage vectors V_7 and V_0, as long as the torque error remains within the predetermined limit of hysteresis band[16-17].

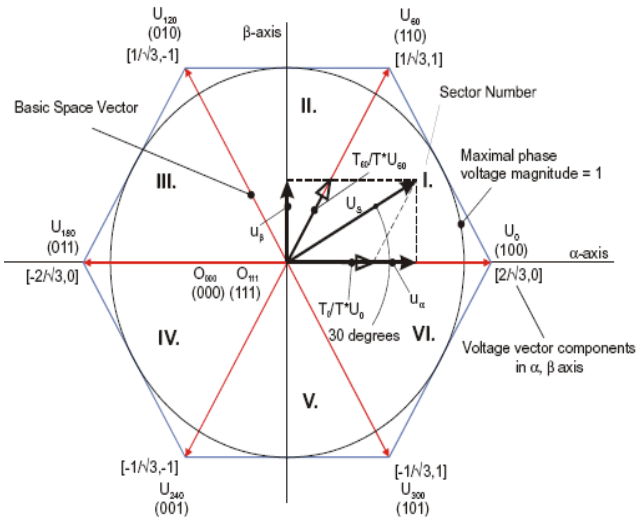

Fig. 3. SVM methodology of DTC.

Finally, the lookup table of DTC-IMD is shown in below:

Table 2: Switching states for DTC.

Φ	τ	S_6	S_5	S_4	S_3	S_2	S_1
	TI	V_2	V_1	V_6	V_5	V_4	V_3
FD	T=	V_7	V_0	V_7	V_0	V_7	V_0
	TD	V_4	V_3	V_2	V_1	V_6	V_5
	TI	V	V	V	V	V	V
FI	T=	V_1	V_6	V_5	V_4	V_3	V_2
	TD	V_0	V_7	V_0	V_7	V_0	V_7

4. LSTM-ANN Controllers

The smart grid's operation and control necessitate data analysis, processing, verification, and data storage. Hence, this study incorporates an LSTM algorithm based on artificial neural networks (ANN) from [15-20]. Additionally, the ANN controller's gains are fine-tuned using a deep learning method. Typically, the signals received from different sections/microgrids in smart grid control units are noisy. To enhance the smart grid's operation, the noisy signal must be filtered. The ANN-based controller unit was designed with memory cells, as illustrated in Figure 4. The fundamental equations are utilized to construct the internal structure of the LSTM system, which is then illustrated in Figure 5. A system is equipped with a machine learning (deep learning) algorithm that adjusts the neuron weights as required. In the analysis, an unidentified noise signal (n_s) is also taken into account, as there could be a disruptive magnetic signal present in the smart grid caused by high voltage and other elements. To mitigate these signals, the LSTM block takes into account the opposite polarity in each element.

$$a_t = \sigma(b_a + h_{t-1} \times w_{ah} + X_t \times w_{ax} \mp n_{sa}) \quad (3)$$

$$f_t = \sigma(b_f + h_{t-1} \times w_{fh} + X_t \times w_{fx} \mp n_{sf}) \quad (4)$$

$$O_t = \sigma(b_o + h_{t-1} \times w_{oh} + X_t \times w_{ox} \mp n_{so}) \quad (5)$$

$$\hat{C}_t = \tanh(b_c + h_{t-1} \times w_{ch} + X_t \times w_{cx} \mp n_{sc}) \quad (6)$$

$$s_t = f_t \otimes s_{t-1} + \hat{C}_t \times a_t \quad (7)$$

$$h_t = \tanh(s_t) \otimes O_t \quad (8)$$

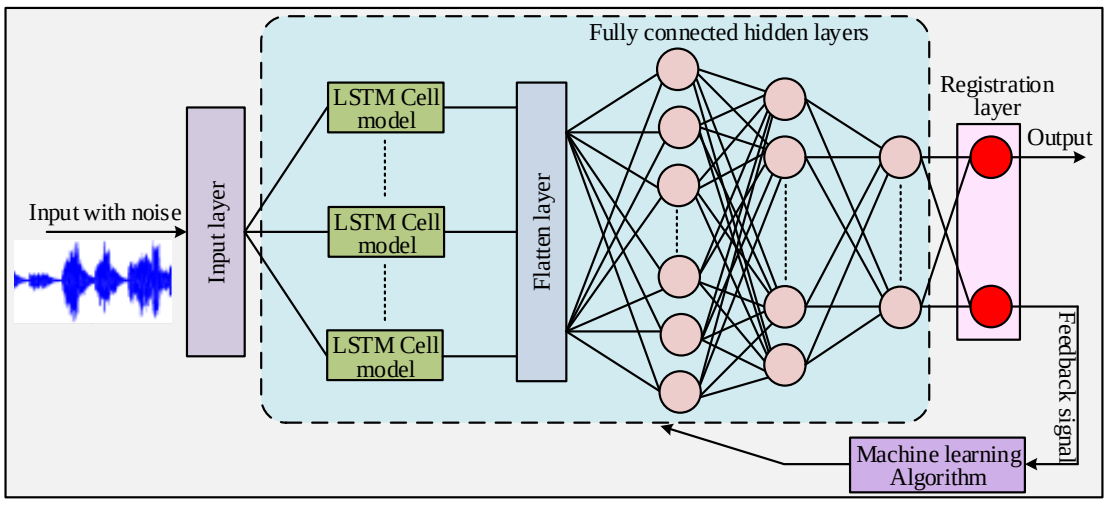

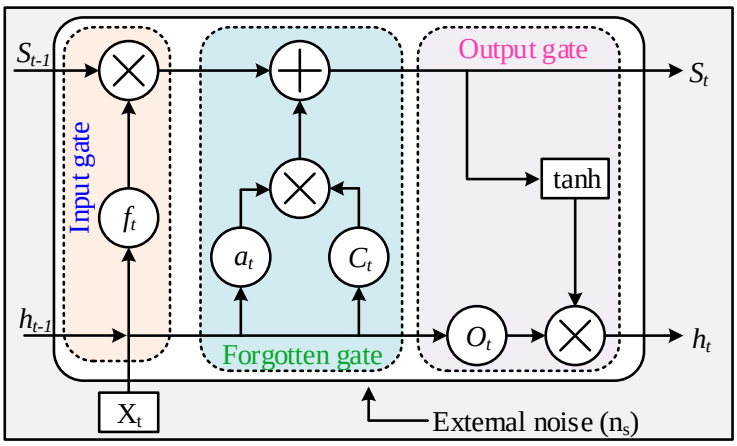

Fig. 5. LSTM Model of a cell.

Algorithm for LSTM System

Inputs: Data sheet of load torque, speed reference, flux, SVM →D_{pp}.

Output: Reference command Signals.

Initialization: 'n' number of torque units are considered← {T_1, T_2, ……T_n}, 'l' number of load torques ← {T_{L1}, T_{L2}, ……T_{Ll}}, etc.

Number of LSTM nodes: N_{LSTMs}.

1: **Procedure** LSTM_Predictions.
2: Identification for Features from D_{pp}.
3: **for** m← l; 0 to n; etc.
4: G_m[m] ← input1(); Y_m[m] ← input2(); etc.
5: **end for**
6: **for** m← l; 0 to n; etc.
7: Normalize T_e, T_L, and other inputs in {0, 1} range.
8: **end for**
9: **for** q←0 to n; l; etc.
10: **if** {T_m[q]; TL_m[q]; etc}.NotValid **then.**
11: {input}←.Interpolate().
12: D_{pp}←duplicate_values.
13: D_p←processed(D_{pp}).
14: **end if**
15: **end for**
16: Repeat for all nodes of LSTM.
17: Output: Predict_best_value_DPP_$LSTM_{layer}$.
18: **end procedure.**

5. Results

This research paper investigates the speed, flux, and torque of SVM-DTC utilizing three LSTM-ANN controllers for an Induction motor. The responses of the generated an reference torques are depicted in Figure 6. In the Simulink model, the motor is subjected to a reference torque of 5.0Nm from time 1.0 to 1.3, 8.0Nm from time 1.3 to 1.8 seconds, and 3.0Nm from 1.8 to 2.0 seconds. The torque produced follows the reference value accurately, with the induction motor speed aligning with the 80rad/s reference speed, as illustrated in Figure 7. The flux trajectory exhibits a smooth curve, as illustrated in Figure 8. For further information on the LSTM and motor parameters, please refer to the appendix (Table-4). It is important to highlight that the utilization of the LSTM-ANN controller results in a reduction in flux ripple, as observed from the stator flux trajectory.

The motor load typically fluctuates due to various factors. Therefore, the efficiency of the suggested system is evaluated against the TS-Fuzzy approach. Additionally, the electromagnetic torque response produced by the motor is illustrated in Figure 9 as the reference torque changes, and it is contrasted with both the TS-Fuzzy and proposed controllers.

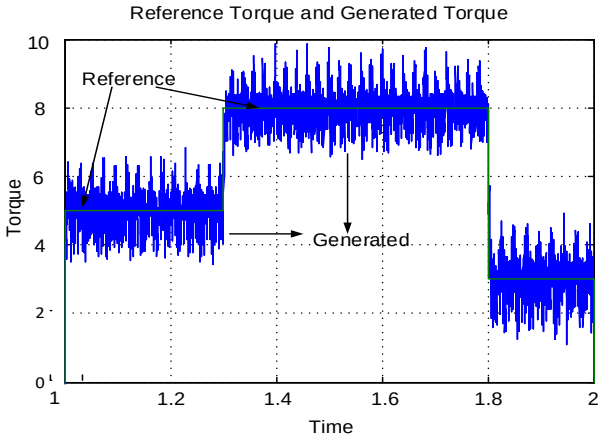

Fig. 6. Responses of reference generated torques.

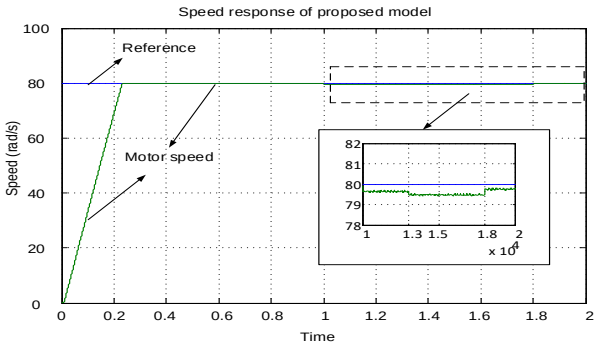

Fig. 7. Responses of reference and generated speeds.

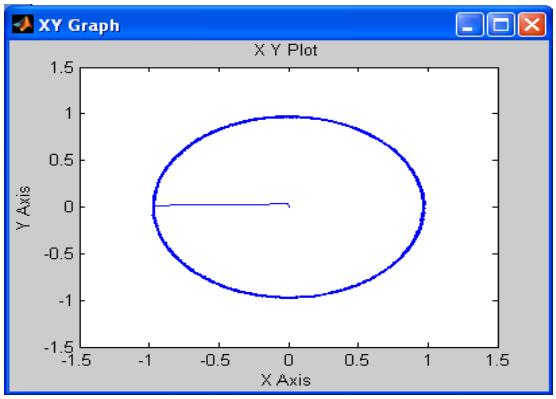

Fig. 8. Stator Flux Trajectory.

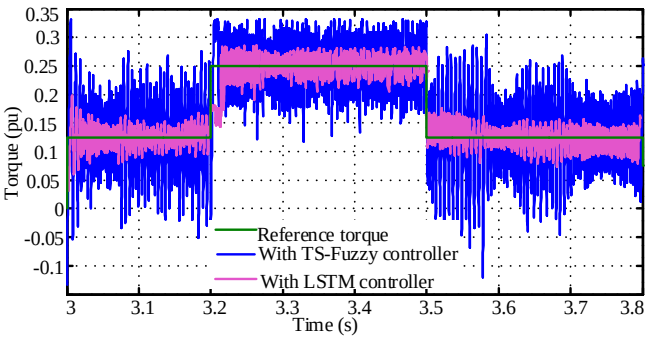

Fig. 9. Response of torque in per unit (pu)

6. Conclusion

The present document presents a DTC drive featuring ANN-LSTM controllers. This controller establishes the target range for torque hysteresis band. The suggested method has shown to result in improved torque and stator flux responses under stable operating conditions. Improved torque and flux ripple characteristics across different speeds result in reduced switching loss and noise levels during motor operation. DTC-SVM with LSTM-ANN controllers is well-suited for electric vehicles because of its numerous benefits, especially in meeting the demanding starting torque needs while minimizing torque fluctuations.

7. Appendix

The DTC approach proposed by LSTM-ANN to minimize torque fluctuations has been widely acknowledged for its effectiveness in solving various issues. Utilizing a LSTM-ANN controller to assess the magnitude of torque hysteresis limit based on the ripples level in torque appears to be a logical decision. Unlike a predetermined value, the amplitude of hysteresis band for torque in this study is determined by a LSTM-ANN controller. After examining sections (II and III), two inputs have been chosen, specifically variations in errors of speed and flux. These inputs are represented by equations 3 and 4 below.

$e_1(k)=\omega(k)-\omega(k-1)$ (9)

$e_2(k)=\Psi_s(k)-\Psi_s(k-1)$ (10)

The stator flux's magnitude is represented by

$$\Psi_s = \sqrt{(\Psi_{\alpha s}^2 + \Psi_{\beta s}^2)} \quad (11)$$

The integration of the crisp output Δb from equation 6 yields the amplitude of the torque hysteresis band.

$b_r(k)=b_r(k-1)+\Delta b_r(k)$ (12)

Parameters of IMD:

Table 3: Various components in IMD.

Parameters	Values
Resistance of Rotor (Rr).	7.55Ω
Resistance of Stator (Rs).	7.83Ω
Inductance of Rotor (Lr).	0.4751H
Inductance of Stator (Ls).	0.4751H
Voltage at DC Link (V_{dc}).	320V.
Mutual Inductance (M).	0.4535H
Pole pairs (2p).	2.0
Friction (B).	0.0021
Inertia (J).	0.06

References

[1] F. Khoucha, M. S. Lagoun, A. Kheloui and M. E. H. Benbouzid, "A Comparison of Symmetrical and Asymmetrical Three-Phase H-Bridge Multilevel Inverter for DTC Induction Motor Drives," in IEEE Transactions on Energy Conversion, vol. 26, no. 1, pp. 64-72, March 2011, doi: 10.1109/TEC.2010.2077296.

[2] Grabowski, P. Z. et al, "A Simple Direct-Torque Neuro Fuzzy Control of PWM-Inverter-Fed Induction Motor Drive", *IEEE Trans. On Industrial Electronics* 47 No. 4 (2000), 863–870.

[3] B. Çavuş and M. Aktaş, "MPC-Based Flux Weakening Control for Induction Motor Drive With DTC for Electric Vehicles," in IEEE Transactions on Power Electronics, vol. 38, no. 4, pp. 4430-4439, April 2023, doi: 10.1109/TPEL.2022.3230547.

[4] J. K. Pandit, M. V. Aware, R. Nemade and Y. Tatte, "Simplified Implementation of Synthetic Vectors for DTC of Asymmetric Six-Phase Induction Motor Drives," in IEEE Transactions on Industry Applications, vol. 54, no. 3, pp. 2306-2318, May-June 2018, doi: 10.1109/TIA.2018.2789858.

[5] V. S. Reddy Chagam and S. Devabhaktuni, "Enhanced Low-Speed Characteristics With Constant Switching Torque-Controller-Based DTC Technique of Five-Phase Induction Motor Drive With FOPI Control," in IEEE Transactions on Industrial Electronics, vol. 70, no. 11, pp. 10789-10799, Nov. 2023, doi: 10.1109/TIE.2022.3227275.

[6] Y. N. Tatte, M. V. Aware, J. K. Pandit and R. Nemade, "Performance Improvement of Three-Level Five-Phase Inverter-Fed DTC-Controlled Five-Phase Induction Motor During Low-Speed Operation," in IEEE Transactions on Industry Applications, vol. 54, no. 3, pp. 2349-2357, May-June 2018, doi: 10.1109/TIA.2018.2798593.

[7] B. Çavuş and M. Aktaş, "A New Adaptive Terminal Sliding Mode Speed Control in Flux Weakening Region for DTC Controlled Induction Motor Drive," in IEEE Transactions on Power Electronics, vol. 39, no. 1, pp. 449-458, Jan. 2024, doi: 10.1109/TPEL.2023.3326383.

[8] M. H. Holakooie, M. Ojaghi and A. Taheri, "Modified DTC of a Six-Phase Induction Motor With a Second-Order Sliding-Mode MRAS-Based Speed Estimator," in IEEE Transactions on Power Electronics, vol. 34, no. 1, pp. 600-611, Jan. 2019, doi: 10.1109/TPEL.2018.2825227.

[9] S. Payami, R. K. Behera and A. Iqbal, "DTC of Three-Level NPC Inverter Fed Five-Phase Induction Motor Drive With Novel Neutral Point Voltage Balancing Scheme," in IEEE Transactions on Power Electronics, vol. 33, no. 2, pp. 1487-1500, Feb. 2018, doi: 10.1109/TPEL.2017.2675621.

[10] D. Mohanraj, J. Gopalakrishnan, B. Chokkalingam and L. Mihet-Popa, "Critical Aspects of Electric Motor Drive Controllers and Mitigation of Torque Ripple—Review," in IEEE Access, vol. 10, pp. 73635-73674, 2022, doi: 10.1109/ACCESS.2022.3187515.

[11] Kang, J. K. et al, "Torque Ripple Minimization Strategy for Direct Torque Control of Induction Motor", *Conf. Rec. IEEE-IAS Annu*. Meeting'98, pp. 438–443 1998.

[12] M. H. Holakooie, M. Ojaghi and A. Taheri, "Direct Torque Control of Six-Phase Induction Motor With a Novel MRAS-Based Stator Resistance Estimator," in IEEE Transactions on Industrial Electronics, vol. 65, no. 10, pp. 7685-7696, Oct. 2018, doi: 10.1109/TIE.2018.2807410.

[13] A. K. Peter, J. Mathew and K. Gopakumar, "A Simplified DTC-SVPWM Scheme for Induction Motor Drives Using a Single PI Controller," in IEEE Transactions on Power Electronics, vol. 38, no. 1, pp. 750-761, Jan. 2023, doi:

10.1109/TPEL.2022.3197362.
[14] M. M. Amin, F. F. M. El-Sousy, O. A. Mohammed, G. A. A. Aziz and K. Gaber, "MRAS-Based Super-Twisting Sliding-Mode Estimator Combined With Block Control and DTC of Six-Phase Induction Motor for Ship Propulsion Application," in IEEE Transactions on Industry Applications, vol. 57, no. 6, pp. 6646-6658, Nov.-Dec. 2021, doi: 10.1109/TIA.2021.3115088.
[15]. U. R. Muduli, B. Chikondra and R. K. Behera, "Space Vector PWM Based DTC Scheme With Reduced Common Mode Voltage for Five-Phase Induction Motor Drive," in IEEE Transactions on Power Electronics, vol. 37, no. 1, pp. 114-124, Jan. 2022, doi: 10.1109/TPEL.2021.3092259.
[16]. P. Kant and B. Singh, "A Sensorless DTC Scheme for 60-Pulse AC-DC Converter Fed 5-Level Six-Leg NPC Inverter Based Medium Voltage Induction Motor Drive," in IEEE Transactions on Energy Conversion, vol. 35, no. 4, pp. 1916-1925, Dec. 2020, doi: 10.1109/TEC.2020.2997240.
[17]. B. Chikondra, U. R. Muduli and R. K. Behera, "An Improved Open-Phase Fault-Tolerant DTC Technique for Five-Phase Induction Motor Drive Based on Virtual Vectors Assessment," in IEEE Transactions on Industrial Electronics, vol. 68, no. 6, pp. 4598-4609, June 2021, doi: 10.1109/TIE.2020.2992018.
[18]. L. Jiang, X. Wang, L. Wang, M. Shao and L. Zhuang, "A hybrid ANN-LSTM based model for indoor temperature prediction," 2021 IEEE 16th Conference on Industrial Electronics and Applications (ICIEA), Chengdu, China, 2021, pp. 1724-1728, doi: 10.1109/ICIEA51954.2021.9516151.
[19]. N. He, L. Liu, D. Chu and C. Qian, "Air Conditioning Cooling Load Prediction Based on LSTM-ANN," 2022 5th International Symposium on Autonomous Systems (ISAS), Hangzhou, China, 2022, pp. 1-6, doi: 10.1109/ISAS55863.2022.9757345.
[20]. A. Amiri, Y. Liang and M. Onyango, "Pioneering Climate Forecasting in Tennessee with LSTM-ANN Machine Learning Model," 2023 IEEE 20th International Conference on Smart Communities: Improving Quality of Life using AI, Robotics and IoT (HONET), Boca Raton, FL, USA, 2023, pp. 126-131, doi: 10.1109/HONET59747.2023.10374680.